Characteristics of mouse intestinal microbiota during acute liver injury and repair following 50% partial hepatectomy

YI SHAO[1], YUANCONG JIANG[1], HUI LI[2], FENG ZHANG[2], ZHENHUA HU[1] and SHUSEN ZHENG[1,2]

[1]Department of Hepatobiliary and Pancreatic Surgery, The First Affiliated Hospital, School of Medicine, Zhejiang University; [2]Key Laboratory of Organ Transplantation, Research Center for Diagnosis and Treatment of Hepatobiliary Diseases, Hangzhou, Zhejiang 310003, P.R. China

Received November 23, 2020; Accepted May 7, 2021

DOI: 10.3892/etm.2021.10385

Abstract. Dysbiosis of the gut microbiota has important roles in various diseases and pathological states of the host. However, the changes of the gut microbiota during partial hepatectomy (PH)-induced acute liver injury have so far remained elusive. The present study investigated the gut microbiome and its related pathways following PH-induced acute liver injury. A total of 50 male C57/BL6 mice were divided into a normal control (NC), sham-operation and liver resection (LR) group (50% PH). Samples were collected at 3 and 14 days post-operation to obtain specimens for the Sham3, Sham14, LR3 and LR14 groups (10 mice/group). Specimens of NC group (n=10) were obtained at the same time as those of Sham3 group. Alanine aminotransferase (ALT) and aspartate aminotransferase (AST) were determined using an automatic chemical analyzer and the gut microbiota was assessed by 16S ribosomal RNA gene sequencing of small intestinal contents. The serum levels of ALT and AST in the LR3 group were significantly increased, while those in the LR14 group were decreased again to near-normal levels. In the LR3 group, the operational taxonomic units, species richness (Chao1) and species diversity (Shannon and Simpson indices) were decreased, although without any significant difference. Furthermore, in the LR3 group, significant Cyanobacteria enrichment and Fusobacteria depletion compared with the NC and Sham3 groups was observed, while in the LR14 group, a significant depletion of the abundance of Verrucomicrobia, Chloroflexi and Deferribacteres compared to the LR3 group was obtained. The abundance of Firmicutes was increased in the LR3 group and decreased again in the LR14 group. However, the abundance of Bacteroidetes and Actinobacteria decreased in the LR3 group and increased again in the LR14 group. The alterations of the gut microbiota at the genus level were also revealed, as significant increases in *Chloroplast*, *Curvibacter*, *Pelomonas*, *Ruminococcaceae* UCG-005 and *Blautia* and a sharp decrease in *Akkermansia* and *Eubacterium coprostanoligenes* were caused by acute liver injury. Furthermore, functional metagenome prediction was performed by Phylogenetic Investigation of Communities by Reconstruction of Unobserved States based on the Greengenes database, revealing alterations in signal transduction, transcription and cell motility, as well as metabolism of amino acids, lipids, glucose, cofactors and terpenoids, and xenobiotics pathways. An improved understanding of the structural and functional changes of the gut microbiota following 50% PH-induced acute liver injury and repair may provide novel strategies for the recovery of hosts undergoing hepatectomy.

Correspondence to: Professor Shusen Zheng, Department of Hepatobiliary and Pancreatic Surgery, The First Affiliated Hospital, School of Medicine, Zhejiang University, 79 Qingchun Road, Hangzhou, Zhejiang 310003, P.R. China
E-mail: shusenzheng@zju.edu.cn

Abbreviations: ALT, alanine aminotransferase; AST, aspartate aminotransferase; CCl4, carbon tetrachloride; KEGG, Kyoto Encyclopedia of Genes and Genomes; LDA, linear discriminant analysis; LEfSe, LDA effect size; LR, liver resection; NMDS, non-metric multidimensional scaling; OTU, operational taxonomic unit; PCA, principal component analysis; PCoA, principal coordinate analysis; PH, partial hepatectomy; PICRUSt, Phylogenetic Investigation of Communities by Reconstruction of Unobserved States; QIIME, Quantitative Insights Into Microbial Ecology; RDP, Ribosomal Database Project; STAMP, statistical analysis of metagenomic profile; TLR, toll-like receptor

Key words: intestinal microecology, gut microbiota, liver resection, 16S rRNA, liver function, liver injury, liver repair, C57/BL6 mice

Introduction

Dysbiosis of the gut microbiota has an important role in various diseases of the host, including obesity, diabetes, inflammatory bowel disease, autoimmune diseases, acute severe pancreatitis, hepatitis, liver cirrhosis, tumors and numerous other pathological states (1-14). A large number of studies focus on gut microbiota changes in liver cirrhosis and acute liver injury [induced by carbon tetrachloride (CCl_4)] (1-6). With the increasing understanding of the relationship between the gut microbiota and host metabolism in cirrhosis, novel methods and approaches may be developed to promote the treatment and prevention of liver cirrhosis (1,2). A study indicated that the abundance of Firmicutes increased and that of Bacteroidetes decreased over time during CCl_4-induced acute liver injury and

that initial alterations in the Firmicute/Bacteroidete ratio may be beneficial to liver repair (6). However, the changes of the intestinal microbiota during partial hepatectomy (PH)-induced acute liver injury have remained elusive. Although 2/3 PH (~70%) is the most studied model of acute liver injury and liver regeneration, resection of ~50% volume of the liver is more frequent in the treatment of liver-associated tumors, as well as living donor liver transplantation and split-liver transplantation in the clinic (15,16). Previous studies suggested that 50% PH caused an immediate and sustained increase in the allospecific cytolytic response in C3H/HeJ mice (17) and caused obvious liver cell acidophilic necrosis and the majority of hepatocyte nuclei to increase in size with vesicular bodies, caryocinesia of nucleoli and stromal inflammatory cell infiltration within 3 days post-operation in C57/BL6 mice (18). In the present study, 50% PH was performed in C57/BL6 mice to mimic the clinical conditions where about half of the liver is surgically resected, and the changes of the gut microbiota and associated pathways during acute liver injury and repair following PH were analyzed. The present study may lay a foundation for further studies on the gut-micbiotaliver metabolic network and aid in establishing the role of probiotics in hepatectomy.

Materials and methods

Animals. A total of 50 male wild-type C57/BL6 mice (body weight, 20-25 g; age, 8 weeks) were purchased from Shanghai SLAC Laboratory Animal Co., Ltd. Mice were raised and maintained in a standardized environment (temperature, 21˚C; humidity, 60%) with a 12-h light/dark cycle and provided with food and water *ad libitum*. The Animal Experimental Ethics Committee of the First Affiliated Hospital, School of Medicine, Zhejiang University (Hangzhou, China) approved all of the procedures. The mice were divided into the following groups: No surgery control group [normal control (NC) group; n=10], sham-operation group (Sham group; n=20) and liver resection (LR) group (50% PH; n=20). All of the mice were kept under the same conditions.

50% PH-induced acute liver injury. The mice were anesthetized by isoflurane inhalation (anesthetic induction on 5% isoflurane at a flow of 10 l/min, followed by anesthetic maintenance using an inspiratory fraction of 1.8-2.2% at a flow of 1 l/min) (19). The caudate lobe, left lateral lobe and left median lobe were then resected to generate the LR model (50% PH) (18,19).

Sample collection. After isoflurane inhalation anesthesia, blood samples were collected by inferior vena cava puncture at 3 and 14 days post-operation. Specimens of the NC group were obtained at the same time as those of Sham3 group. Following exsanguination, the livers were harvested, fixed with 4% paraformaldehyde and paraffin-embedded for histological analysis. The small intestinal contents were precisely dissected and harvested, frozen in liquid nitrogen and preserved at -80˚C until analysis. Serum was acquired by centrifugation of the blood samples at 2,500 x g for 20 min at 4˚C and kept at -80˚C until analysis.

Biochemical analysis and liver histology. Serum alanine aminotransferase (ALT) and aspartate aminotransferase (AST) were determined using an automatic chemistry analyzer (Mindray BS-220; Mindray Bio-medical Electronics Co., Ltd.) according to the manufacturer's protocol. For histopathological analysis, paraffin-embedded liver samples were sectioned (5 μm thickness) and stained with H&E. Images were acquired (original magnification, x400) using a digital colour camera (DP20; Olympus Corporation).

Intestinal microbiota analysis by 16S ribosomal (r)RNA gene sequencing. The small intestinal contents from all the mice were subjected to analysis of the microbial diversity. DNA was extracted from all samples using an E.Z.N.A.® Stool DNA Kit (cat. no. D4015-02; Omega Biotek). The V3-V4 region of the 16S rRNA gene was amplified with primers as follows: 341 Forward, 5'-CCTACGGGNGGCWGCAG-3'; and 805 Reverse, 5'-GACTACHVGGGTATCTAATCC-3'. PCR amplification was performed in a reaction mixture with a total volume of 25 μl, including 25 ng of purified DNA, 12.5 μl PCR Premix (Phusion Hot start flex 2X Master Mix; cat. no. M0536L; New England Biolabs, Inc.), 2.5 μl of each primer and PCR-grade water to adjust the volume. The PCR cycling conditions consisted of an initial denaturation step at 98˚C for 30 sec, 32 cycles of denaturation at 98˚C for 10 sec, annealing at 52˚C for 30 sec and extension at 72˚C for 45 sec, and a final extension step at 72˚C for 10 min (20). PCR products were purified using AMPure XT beads (cat. no. A63880; Beckman Coulter Genomics), quantified with a Qubit dsDNA HS Assay kit (cat. no. Q32854; Invitrogen; Thermo Fisher Scientific, Inc.), pooled in equimolar ratios and then sequenced with a 2x300 bp paired end protocol on a MiSeq PE300 platform (Illumina, Inc.).

Data analysis. Raw sequencing data were merged using the Fast Length Adjustment of SHort reads software v1.2.8 (http://ccb.jhu.edu/software/FLASH/) based on overlapping bases. Quality filtering of the raw tags was performed to obtain the high-quality clean tags according to fqtrim v0.9.4 (https://zenodo.org/record/20552#.YMF-26aS3IU). Chimeric sequences were filtered using Vsearch software v2.3.4 (https://zenodo.org/record/198592#.YMGAHaaS3IV). The processed sequences were assigned to the same operational taxonomic units (OTUs) at 97% identity (21,22). Representative sequences were selected for each OTU and annotated against the Ribosomal Database Project (RDP) classifier (http://rdp.cme.msu.edu/) and National Center for Biotechnology Information (NCBI)-16s database (https://www.ncbi.nlm.nih.gov/gene/27471). The effective sequences were analyzed by Quantitative Insights Into Microbial Ecology (QIIME) software v1.8.0 (23,24). α-diversity, including the indexes of Chao1, Observed OTUs, Goods coverage, Shannon and Simpson, was calculated by QIIME to analyze the complexity of species diversity for a sample (23,24). β-diversity, referring to the species diversity between different samples, including principal component analysis (PCA), unweighted UniFrac principal coordinate analysis (PCoA) and unweighted UniFrac distance-based non-metric multidimensional scaling analysis (NMDS), were calculated by QIIME (23,24). Linear discriminant analysis (LDA) effect size (LEfSe) was applied to estimate the characteristic types of bacteria of each group (25). Metagenome prediction and functional differences among

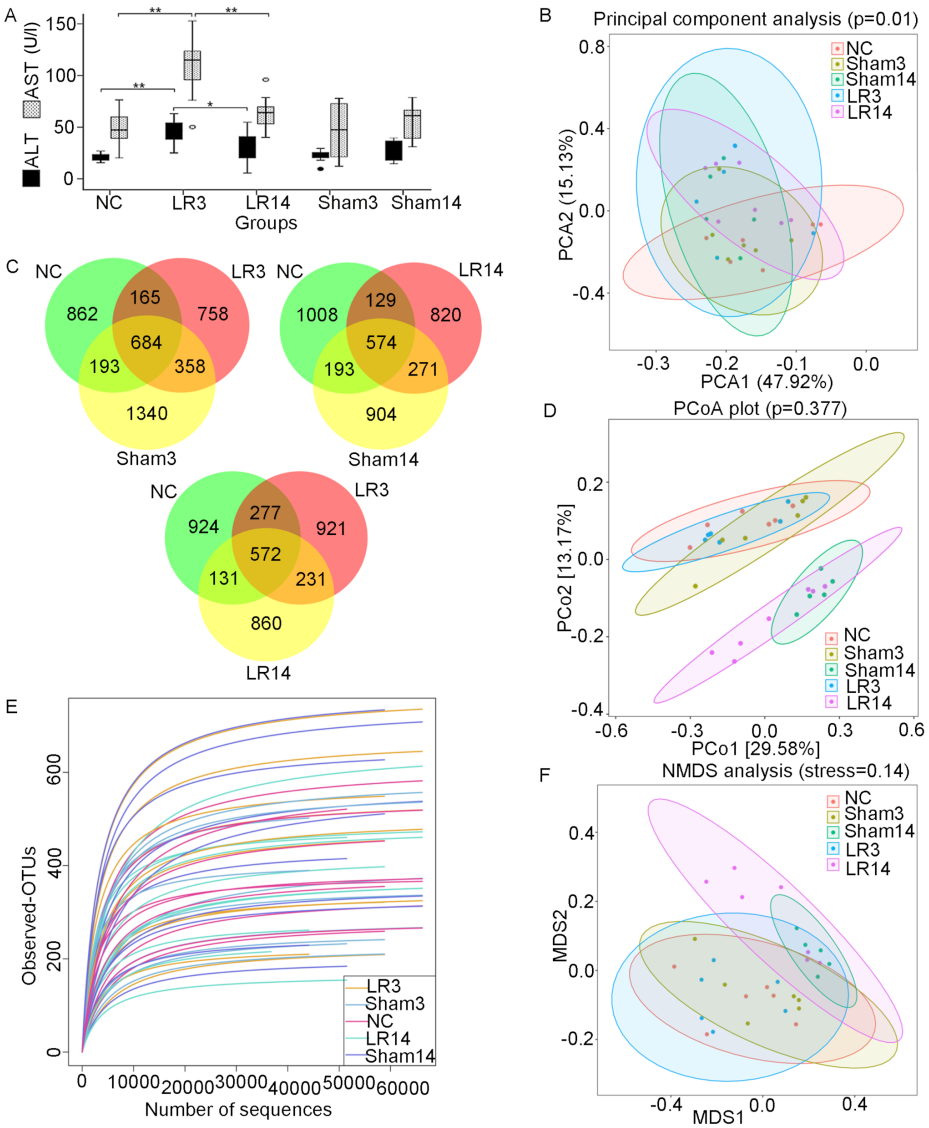

Figure 1. Changes in liver function and gut microbiota following 50% partial hepatectomy. (A) Liver ALT and AST levels. Values are expressed as the median (interquartile range) (n=10 per group). *P<0.05, **P<0.01 according to ANOVA with LSD post-hoc test. (B) PCA of the bacterial community of the small intestinal contents of the mice. (C) Three-part Venn diagrams display the OTUs shared among the groups. The numbers in the diagrams represent the numbers of unique OTUs in each group or shared between groups as their areas intersect. (D) Unweighted UniFrac distance-based PCoA plots. (E) Rarefaction curves. (F) Unweighted UniFrac distance-based NMDS. Groups: NC, normal control; LR3, 3 days post-liver resection; LR14, 14 days post-liver resection; Sham3, 3 days post-sham operation; Sham14, 14 days post-sham operation; OTU, operational taxonomic unit; PCA, principal component analysis; PCoA, principal coordinate analysis; NMDS, non-metric multidimensional scaling; ALT, alanine aminotransferase; AST, aspartate aminotransferase.

groups were investigated by the Phylogenetic Investigation of Communities by the Reconstruction of Unobserved States (PICRUSt) software based on the Greengenes database (26). The output files were further analyzed by STatistical Analysis of Metagenomic Profile (STAMP) software (27).

Statistical analysis. Values are expressed as the mean ± standard deviation or the median (interquartile range) and variables were compared between two groups by Student's t-test (normal distribution and equal variance) or nonparametric Mann-Whitney U-test (non-normal distribution). Comparisons among more than two groups were performed by ANOVA with LSD post-hoc test or nonparametric Kruskal-Wallis H-test. A two-tailed P<0.05 was considered to indicate statistical significance. Data were analyzed by SPSS 22.0 (IBM Corporation) and R software (v3.5.1; 2018; R Development Core Team).

Results

Acute liver injury and repair following 50% PH. A total of 50 mice were used in the present study. The 50% PH surgery was performed in 20 mice and the sham operation in 20 mice, while the 10 remaining mice were used as NC. In each group, 10 mice were sacrificed 3 days post-operatively and the other 10 were sacrificed at 14 days post-operatively. Animals from the NC group were sacrificed at the same time as those of Sham3 group. None of the mice was accidentally dead after the operation. Serum ALT and AST were tested for each mouse (Fig. 1). The mice in the group sacrificed 3 days post-50% PH (LR3 group) exhibited acute liver injury compared with those in the group sacrificed 3 days post-sham operation (Sham3 group) and the NC group, while the liver function of the mice sacrificed 14 days post-50%

PH (LR14 group) had partially recovered (Fig. 1A). Liver histology slides of group LR3 exhibited swelling of certain hepatocytes with acidophilic necrosis and the majority of hepatocytes had single enlarged, double or multiple nuclei, prominent nucleoli caryocinesia and vesicular bodies. In the LR14 group, single enlarged or double nuclei were still present but with less prominent acidophilic bodies in most hepatocytes (Fig. 2).

Overall structural changes of intestinal microbiota following 50% PH. The V3-V4 region of the 16S rRNA was sequenced on the Illumina MiSeq platform and a total of 4,050,657 raw reads were obtained. After multiple paired-ends joining, quality trimming and filtering steps of the raw sequencing data, a total of 3,738,823 high-quality sequences were acquired, with an average of 74,776 (range, 54,900-93,663) sequences per sample. Specifically, 717,489, 775,830, 711,428, 777,509 and 756,567 sequences were acquired from the NC, Sham3, Sham14, LR3 and LR14 group, respectively. All of the sequences were clustered into 5,799 OTUs and aggregated into 42 phyla and 815 genera. There were 1,904 species-level OTUs in the NC group and 2,575, 1,942, 1,992 and 1,794 OTUs in the Sham3, Sham14, LR3 and LR14 group, respectively (Table I). Three-part Venn diagrams were generated to display the overlaps among groups, demonstrating that 684 of the total 4,387 OTUs were shared among the NC, Sham3 and LR3 groups, 572 out of 3,630 OTUs were shared among the NC, LR3 and LR14 group, and 574 out of 3,899 OTUs were shared among the NC, Sham14 and LR14 groups (Fig. 1C). Of note, the LR groups had the lowest number of unique OTUs in their comparisons.

Microbiota community richness and diversity changes following 50% PH. Analysis of the α-diversity indicated that the observed OTUs and species richness (Chao1) were lower in the LR groups than those in the Sham group but without any significant difference (Table I). The species diversity (Shannon and Simpson indices) was also lower in the LR groups, while that in the LR14 group was slightly higher than that in the LR3 group (Shannon: 4.3405 vs. 4.2855, P=0.22; Simpson: 0.8393 vs. 0.8334, P=0.48; Table I). Good coverage of all samples was >99.8% and rarefaction curves of all the samples approached a plateau (Fig. 1E), indicating sufficient sequencing for the coverage of all OTUs. The results indicated that after LR, the species richness was steadily decreased (Chao1 and observed OTUs) over time. Of note, the trend of the changes in the Sham group was more obvious than that in the LR group. Furthermore, LR decreased the species diversity, and conversely, the sham operation increased it (Table I). We hypothesize that anesthesia, surgical trauma and stress of the sham operation could increase the species diversity, while acute liver injury of the LR could decrease the species diversity.

Furthermore, β-diversity was assessed by PCA, PCoA and NMDS based on the unweighted UniFrac distances between the samples (23,24). PCA revealed that the LR groups were distinguished from the NC group (Fig. 1B). PCoA indicated that most of the samples from the NC, Sham3 and LR3 groups were clustered together, while they were separated from the Sham14 and LR14 groups (Fig. 1D). NMDS analysis provided a similar result (Fig. 1F).

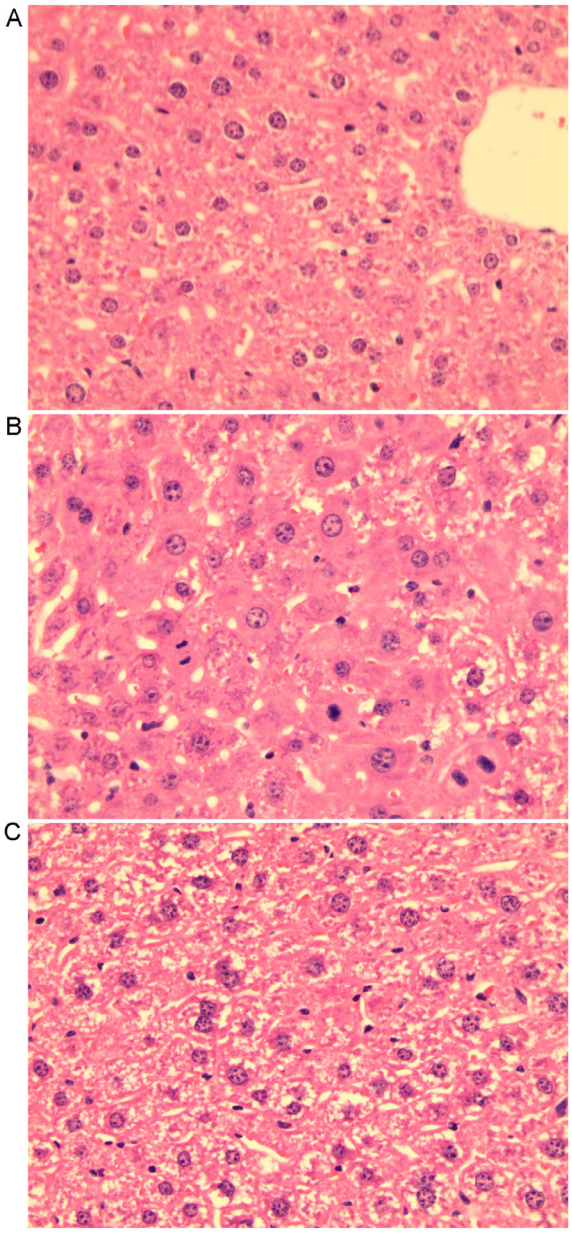

Figure 2. Histological examination of the livers following 50% PH. (A) Liver histology slide from the sham-operation group displaying clear hepatic lobules, radial hepatic cord and clear hepatic sinusoid. (B) Liver histology slide of 50% PH mice 3 days post-operation displaying cloudy swelling of certain hepatocytes with acidophilic necrosis and the majority of hepatocytes with single enlarged, double or multiple nuclei, prominent nucleoli and cytoplasmic acidophilic bodies. (C) Liver histology slide of 50% PH mice 14 days post-operation displaying single enlarged or double nuclei but less prominent acidophilic bodies (H&E staining; magnification, x400). PH, partial hepatectomy.

Alterations of taxonomy community at the phylum level following 50% PH. The 16S rRNA amplicon libraries from the small intestinal contents were sequenced and established to characterize the alterations in gut microbiota associated with 50% PH-induced acute liver injury and repair. At the phylum level, the 5 dominant bacterial phyla were Firmicutes, Proteobacteria, Bacteroidetes, Actinobacteria and Cyanobacteria, accounting for >90% of all sequences in all groups (Figs. 3 and 4). Relative abundances of the intestinal microbiota at the bacterial phylum level among different

Table I. α-Diversity estimation for each group from the pyrosequencing analysis.

Groups	OTUs (n)	Good coverage (%)	Chao1	95% CI	Observed OTUs	95% CI	Shannon	Simpson
NC	1904	99.94	384	298.6-469.0	376	299-452	4.0611	0.8071
Sham3	2575	99.92	497	409.1-588.2	486	401-574	4.7900	0.8681
LR3	1992	99.95	391	329.2-466.0	384	316-456	4.2855	0.8334
Sham14	1942	99.96	403	287.4-516.2	397	284-518	4.5358	0.8404
LR14	1794	99.95	362	287.6-447.3	355	281-439	4.3405	0.8393

OTU, operational taxonomic unit; CI, confidence interval. Groups: NC, normal control group; Sham3, 3 days post sham-operation group; LR3, 3 days post-liver resection group; Sham14, 14 days post-sham operation group; LR14, 14 days post-liver resection group.

groups were presented in a hierarchical clustering heatmap (Fig. 3A). LR led to an increase in Firmicute abundance but decreases in Bacteroidetes and Actinobacteria, compared with the Sham group, but without any statistically significant difference (Figs. 3A and B and 4A and C). In group LR3, significant Cyanobacteria enrichment and Fusobacteria depletion in comparison with the NC and Sham groups was observed (P=0.03 and 0.02, respectively; Fig. 5A). Then in the liver repair phase (LR14), Cyanobacteria were enriched and Verrucomicrobia were depleted compared with the NC and Sham groups (P=0.04 and <0.001, respectively; Fig. 5A). Furthermore, compared with those in the LR3 group, mice in the LR14 group exhibited a decrease in Firmicute abundance and increases in Proteobacteria, Bacteroidetes, Actinobacteria and Cyanobacteria, but without any statistical significance (Figs. 3A and B and 4A and C). In the LR14 group, significantly depleted Verrucomicrobia and Chloroflexi abundance was observed in comparison to the LR3 group (P=0.01 and 0.03, respectively; Fig. 5A).

Alterations of taxonomy community at the genus level following 50% PH. At the genus level, the 5 most abundant bacterial genera were distributed in phyla as follows: Two Firmicutes (*Lactobacillus* and *Streptococcus*), one Bacteroidete (*Muribaculaceae*) and two Proteobacteria (*Pseudomonas* and *Brevundimonas*) (Fig. 4B-D). The remaining 4 of the 9 most abundant bacterial genera were *Candidatus arthromitus*, *Mitochondria*, *Sandaracinobacter* and *Enterorhabdus*, which belong to the phyla Firmicutes, Proteobacteria, Proteobacteria and Actinobacteria, respectively (Figs. 3C and 4C and D). In the LR3 group, significant increases in *Chloroplast*, *Curvibacter*, *Pelomonas*, *Ruminococcaceae* UCG-005 and *Blautia* (belonging to the phyla Cyanobacteria, Proteobacteria, Proteobacteria, Firmicutes and Firmicutes, respectively) but a sharp decrease in *Akkermansia* and *Eubacterium coprostanoligenes* (belonging to the phyla Verrucomicrobia and Firmicutes, respectively) were observed compared with the Sham and NC groups (P<0.05; Fig. 5B). In the liver repair phase (LR14 group), *Candidatus arthromitus*, *Chloroplast* and *Kineococcus* (belonging to the phyla Firmicutes, Cyanobacteria and Actinobacteria, respectively) were enriched, while *Escherichia-Shigella* and *Faecalibacterium* (belonging to the phyla Proteobacteria and Firmicutes, respectively) were depleted compared with the Sham and NC groups (P<0.05; Fig. 5B). Compared with those in group LR3, mice in group LR14 exhibited significant increases in *Candidatus arthromitus* and *Mucispirillum* (belonging to the phyla Firmicutes and Deferribacteres, respectively) but significant decreases in *Ruminococcus*, *Subdoligranulum*, *Romboutsia*, *Clostridium sensu stricto 1* and *Paenibacillus* (phylum, Firmicutes), *Bifidobacterium*, *Corynebacterium* and *Streptomyces* (phylum, Actinobacteria), *Nevskia* and *Escherichia-Shigella* (phylum, Proteobacteria), *Chryseobacterium* and *Parabacteroides* (phylum, Bacteroidetes) and *Akkermansia* (phylum, Verrucomicrobia) were obtained (P<0.05; Fig. 5B).

Specific bacterial taxa with significant changes in relative abundance following 50% PH. LEfSe analysis was used to distinguish more specific bacterial taxa whose relative abundance was significantly different among the NC, Sham and LR groups (25), revealing that in the LR3 group, the microbiota had an increased abundance in Oxyphotobacteria at the class level, Chloroplast at the order level, Chloroplast at the family level, *Chloroplast* and *Curvibacter* at the genus level and *Chloroplast* sp. and *Curvibacter* sp. at the species level (distinct from NC and Sham, LDA scores >3; Fig. 6A). This analysis also revealed that in the LR14 group, the microbiota was enriched in Cyanobacteria at the phylum level, Oxyphotobacteria at the class level, Chloroplast at the order level, Clostridiaceae 1, Chloroplast and Rhodanobacteraceae at the family level, *Candidatus arthromitus*, *Chloroplast* and *Tahibacter* at the genus level and *Candidatus arthromitus* sp., *Chloroplast* sp. and *Tahibacter* sp. at the species level (distinct from NC and Sham, LDA scores >3; Fig. 6B). Furthermore, Fig. 6C provides the differential taxa between the LR3 and LR14 groups determined using the LEfSe analysis method, revealing that in the LR14 group, the microbiota exhibited an increased abundance in Clostridiaceae 1 at the family level, *Candidatus arthromitus, Eubacterium nodatum* and *Ruminococcaceae NK4A214* at the genus level and *Candidatus arthromitus* sp., *Eubacterium nodatum* sp., *Papillibacter* sp. and *Ruminococcaceae NK4A214* sp. at the species level (distinct from LR3, LDA scores >3; Fig. 6C). Collectively, all of these results demonstrated that the gut microbiota may have an important role in the acute liver injury and repair following 50% PH.

Potential functional changes of the gut microbiome following 50% PH. The metagenome Kyoto Encyclopedia of Genes

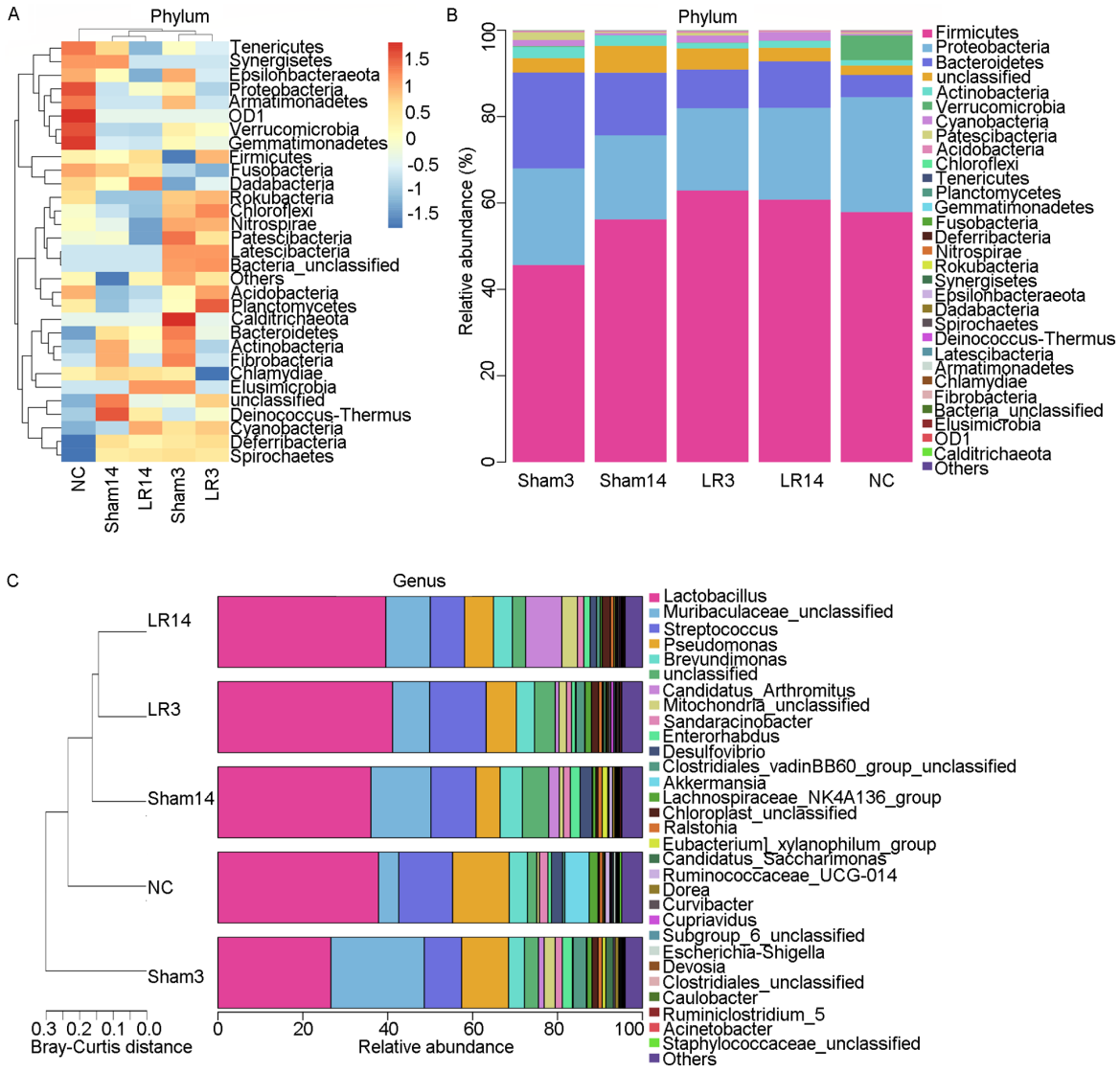

Figure 3. Altered microbial community composition following 50% partial hepatectomy-induced acute liver injury. (A) Hierarchical clustering heatmap of the top 30 bacterial phyla of each group. (B) Stacked bar charts indicating the relative abundances of the gut microbiota at the bacterial phylum level. (C) Hierarchical clustering stacked bar charts of the top 30 bacterial genera of each group. Groups: NC, normal control; LR3, 3 days post-liver resection; LR14, 14 days post-liver resection; Sham3, 3 days post-sham operation; Sham14, 14 days post-sham operation; OD1, candidate phylum OD1 bacteria (also referred to as Parcubacteria).

and Genomes (KEGG) orthologies of the 50 samples were predicted with PICRUSt software based on the Greengenes database (26). Then KEGG orthologies were collapsed to the pathway level (KEGG level 3) by PICRUSt. The differences in KEGG pathways between groups were determined by STAMP (27). Fig. 7 provides the statistically significant KEGG pathways compared between pairs of groups (LR3 vs. Sham3, LR14 vs. Sham14 and LR3 vs. LR14). In group LR3, a significant enhancement of the 'myo-, chiro- and scillo-inositol degradation' and 'isoprene biosynthesis II (engineered)' pathways, but a significant decline of the 'incomplete reductive TCA cycle' pathway, compared to the Sham3 group was obtained (Fig. 7A). However, in group LR14, enhancement of 'anhydromuropeptides recycling', 'GDP-mannose biosynthesis' and 'urea cycle' pathways, but a decline of the 'superpathway of L-isoleucine biosynthesis I' pathway in comparison with the Sham14 group was present (Fig. 7B). Compared to the LR3 group, the LR14 group exhibited significant enhancements in the 'GDP-mannose biosynthesis' and 'urea cycle' pathways but decreases in numerous other pathways, including 'cob(II)yrinate a,c-diamide biosynthesis I (early cobalt insertion)', 'superpathway of (Kdo)2-lipid A biosynthesis', 'superpathway of L-tryptophan biosynthesis', 'enterobactin biosynthesis' and 'superpathway of chorismate metabolism' (Fig. 7C).

Discussion

The intestinal microecology has critical roles in regulating metabolic processes (7,8), modulating immunity (9,10) and protecting the host against pathogenic microbes (11) and is considered an ignored endocrine organ (1,7,8). Signals from the intestinal microbiota have been related to the maintenance of healthy host function and prevention of various diseases, including obesity, diabetes, inflammatory bowel disease, liver disease, allergy and cancer (1-14).

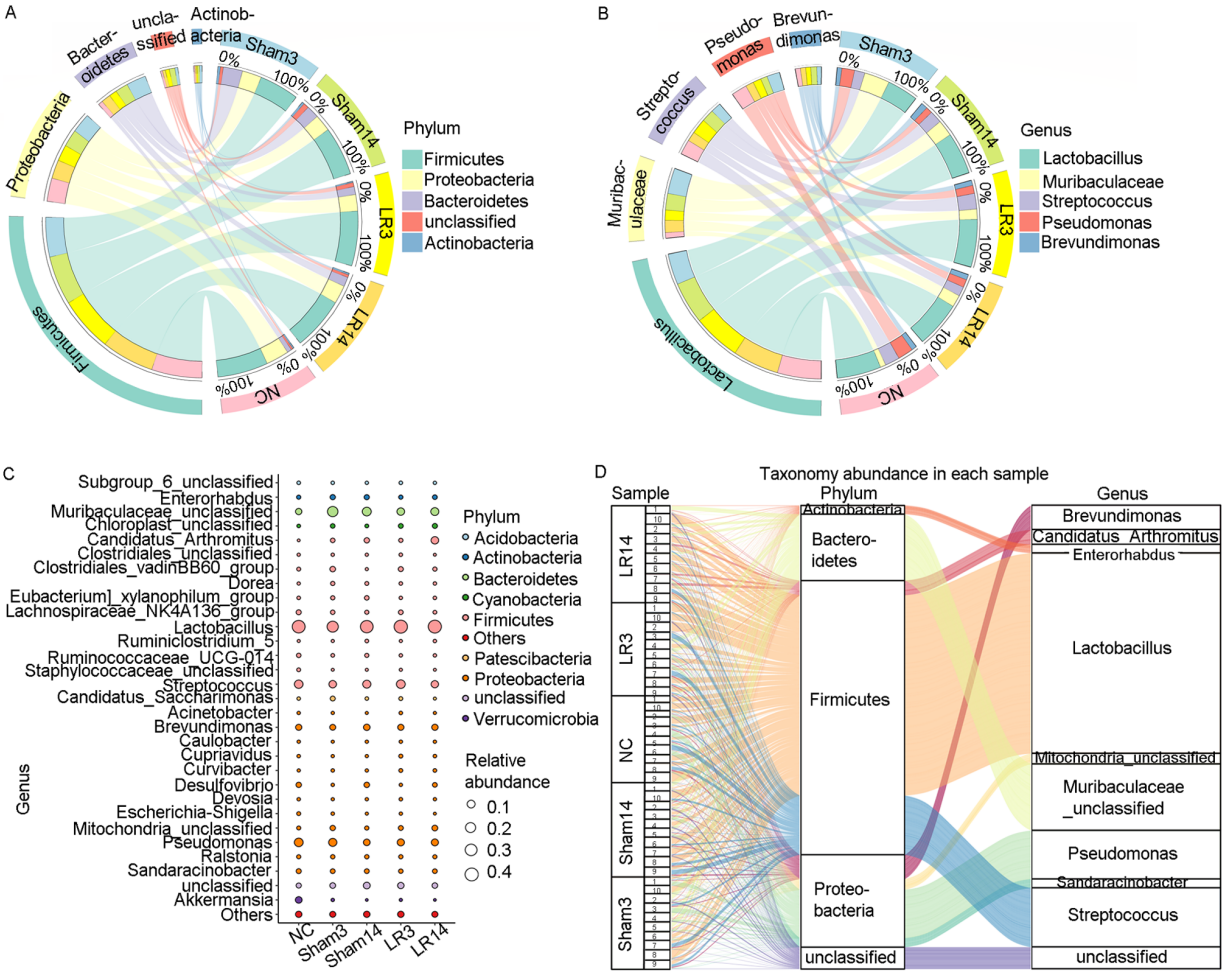

Figure 4. Gut microbiota changes at the bacterial phylum level and genus level following 50% partial hepatectomy. (A) Circos plot displaying the abundance of the 5 dominant bacterial phyla in each group. (B) Circos plot displaying the abundance of the 5 dominant bacterial genera in each group. (C) Bubble chart indicating the relative abundance of bacterial phyla and bacterial genera for each group. (D) Sankey plot providing the relative abundance of bacterial phyla and bacterial genera for each sample. Groups: NC, normal control; LR3, 3 days post-liver resection; LR14, 14 days post-liver resection; Sham3, 3 days post-sham operation; Sham14, 14 days post-sham operation.

Studies have revealed that changes in the intestinal microbiota have an important role in the development of liver diseases (1-6,13). The diversity, richness and function of the intestinal microbiota have been associated with hepatitis B, liver cirrhosis and acute liver injury (1-6). The intestinal microbiota was determined to influence the host immune response to hepatitis B virus and may determine whether acute or chronic hepatitis B occurs (2). Patients with chronic hepatitis B and cirrhosis exhibited significantly increased *Enterococcus* and *Enterobacteriaceae* levels, but markedly decreased *Bifidobacteria* and *Lactobacillus* levels compared with healthy subjects (2,3). To a certain extent, liver cirrhosis may be caused by bacterial products from the intestine (3,4). Overgrowth of harmful bacteria in the intestine leads to increased mucosal permeability, which causes bacterial or endotoxin translocation and thus activate the liver's innate immune system (1,2,13). The lipopolysaccharide-toll-like receptor (TLR) 4 pathway and the unmethylated CpG DNA-TLR9 pathway may be 2 important related immune mechanisms (2). Serum lipids (phospholipids, free fatty acids, eicosapentaenoic acid, arachidonic acid and docosahexaenoic acid) were indicated to have significant correlations with *Enterococcus*, *Enterobacteriaceae*, *Bifidobacterium*, *Bacteroides*, *Lactobacillus* and *Candida* (5). These correlations differed among normal liver, liver fibrosis and liver cirrhosis groups, suggesting that chronic liver disease itself alters the intestinal flora-associated fatty acid metabolism (5). The intestinal microbiota produces a variety of compounds that have critical roles in regulating the activity of the liver (1,2). Studies on CCl_4-induced acute liver injury revealed that Firmicute abundance increased and Bacteroidetes decreased over time, and initial alterations in the Firmicute/Bacteroidete ratio may be beneficial to liver repair (6). However, the changes of the intestinal microbiota during PH-induced acute liver injury had remained elusive. In order to simulate the clinical situation as much as possible, a 50% PH model was selected for the present study. Regardless of the type of liver damage, the general association between liver damage and changes in the microbiota was demonstrated in the present study.

In the present study, changes in the intestinal microbiota following 50% PH-induced acute liver injury and repair were assessed. α-Diversity analysis suggested that LR induced a reduction of observed OTUs, species richness (Chao1) and species diversity (Shannon and Simpson indices), although

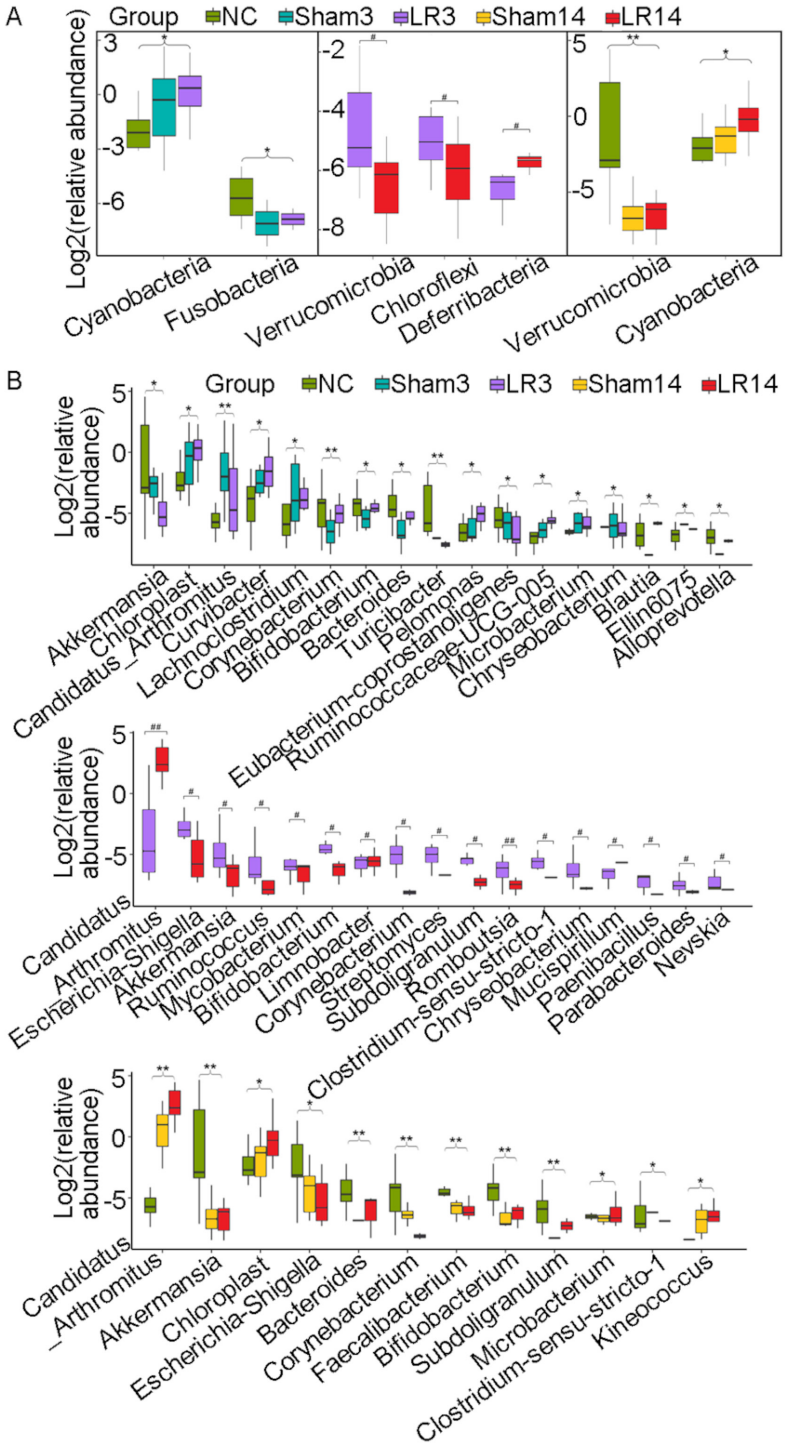

Figure 5. Box plots displaying differences in the gut microbiota following 50% partial hepatectomy at the bacterial (A) phylum level and (B) genus level. Values are expressed as the median (interquartile range) (n=10 per group). $^{\#}$P<0.05, $^{\#\#}$P<0.01, nonparametric Mann-Whitney U-test; *P<0.05, **P<0.01, nonparametric Kruskal-Wallis H-test, the statistical significance is indicated among all three groups compared. Groups: NC, normal control; LR3, 3 days post-liver resection; LR14, 14 days post-liver resection; Sham3, 3 days post-sham operation; Sham14, 14 days post-sham operation.

without any significant differences. An increase in Firmicute abundance and decreases in Bacteroidetes and Actinobacteria were detected in association with LR and alterations of the Firmicute/Bacteroidete ratio were indicative of diverse disease processes (28). LR significantly induced Cyanobacteria enrichment over time. In contrast to acute liver injury, liver repair led to a significant depletion of Verrucomicrobia, Chloroflexi and Deferribacteres, suggesting that these bacterial phyla may also have indispensable roles in 50% PH. In addition, at the genus level, LR3 led to significant upregulation of *Chloroplast*, *Curvibacter*, *Pelomonas*, *Ruminococcaceae* UCG-005 and *Blautia* but downregulation of *Akkermansia* and *Eubacterium coprostanoligenes* compared with the Sham and NC groups. Obviously, acute liver injury caused overgrowth of intestinal pathogenic microorganisms and the fading of intestinal beneficial bacteria. The differences in bacterial

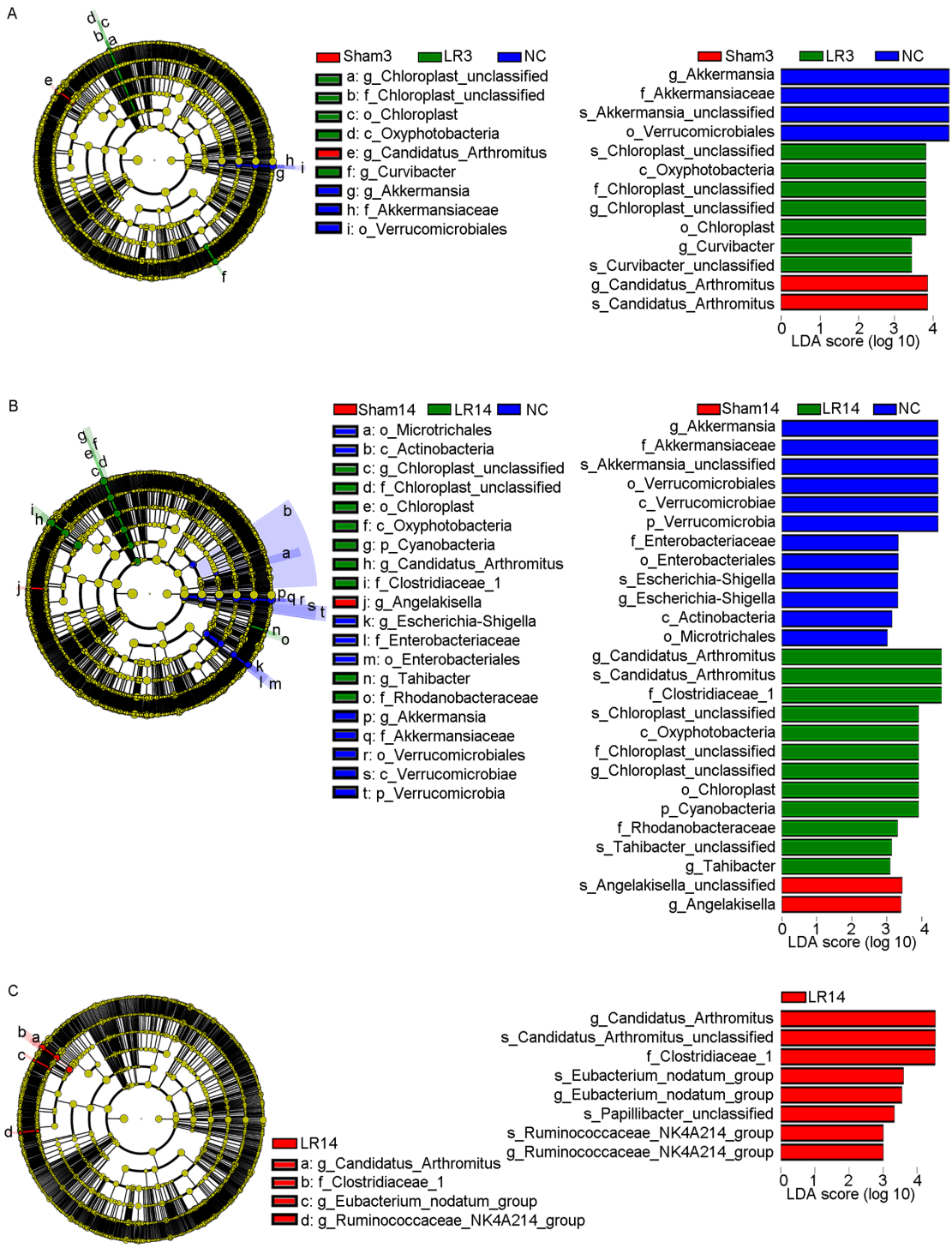

Figure 6. LEfSe (LDA scores >3) method identifies characteristic taxa following 50% partial hepatectomy. (A) LEfSe among the LR3, Sham3 and NC groups. (B) LEfSe among the LR14, Sham14 and NC groups. (C) LEfSe between the LR3 and LR14 groups. Groups: NC, normal control; LR3, 3 days post-liver resection; LR14, 14 days post-liver resection; Sham3, 3 days post-sham operation; Sham14, 14 days post-sham operation; LDA, linear discriminant analysis; LEfSe, LDA effect size.

genera between the LR14 and LR3 groups suggested that in the liver repair phase, the amount of pathogenic microorganisms decreased, while that of beneficial bacteria increased, resulting in the restoration of the intestinal microecological balance.

Among the significantly different bacterial taxa, previous studies also revealed that Ruminococcaceae exhibited a higher transcriptional activity than abundance in ulcerative colitis patients (14) and also require anaerobic conditions and carbohydrate energy sources from dietary fibre (29). Cyanobacteria and chloroplasts were responsible for pathways related to photosynthesis (29). *Clostridium*, known as pathogenic bacteria (30), have an important role in mice with obesity (31,32). *Akkermansia*, regarded as mucus-degrading bacteria, which were able to adhere to the gut epithelium and reinforce enterocyte layer integrity *in vitro* (33) and initiate mucus degradation to generate oligosaccharides and

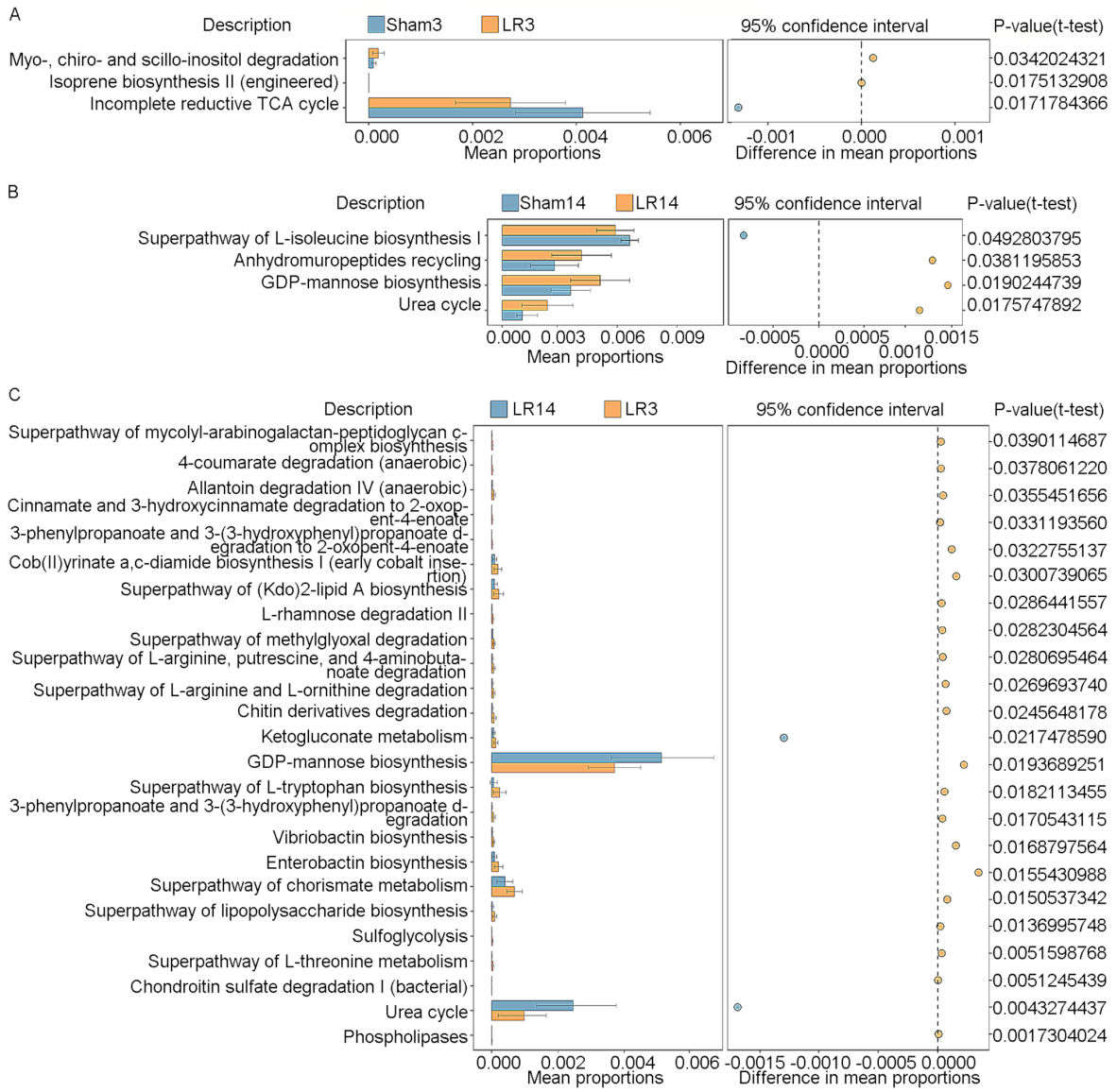

Figure 7. Functional divergences of gut microbiota are illustrated by KEGG pathway analysis predicted through Phylogenetic Investigation of Communities by the Reconstruction of Unobserved States. Statistically significant KEGG pathways between the groups were determined by STatistical Analysis of Metagenomic Profile software (White's nonparametric t-test, P<0.05). Significant differences in KEGG pathways were identified between (A) the LR3 and Sham3 groups, (B) LR14 and Sham14 groups and (C) LR3 and LR14 groups. Groups: LR3, 3 days post-liver resection; LR14, 14 days post-liver resection; Sham3, 3 days post-sham operation; KEGG, Kyoto Encyclopedia of Genes and Genomes.

acetate, evoking colonized bacterial growth and resistance to pathogenic microorganisms *in vivo*, were beneficial for the composition of the mucus-related microbiota (34). An increased *Akkermansia* population in the gut microbiota was associated with the improvement of metabolic syndrome and prevention of diet-induced obesity, insulin resistance and intestinal inflammation in high-fat diet-fed mice (35).

Functional KEGG pathway analysis provided the specific and distinct pathways of the gut microbiome associated with acute liver injury and repair following 50% PH, revealing that the potential functions of the gut microbiota differed significantly during the liver injury and repair phase. Acute liver injury led to the upregulation of biosynthesis of isoprene, heme, geranylgeranyldiphosphate and factor 420, and enhancement of degradation of N-acetylneuraminate, myo-inositol and myo-, chiro- and scillo-inositol, associated with increased *Chloroplast*, *Curvibacter*, *Pelomonas*, *Ruminococcaceae UCG-005* and *Blautia* abundance as compared to the Sham3 group. Furthermore, acute liver injury induced downregulation of glycolysis V, formaldehyde assimilation II, biosynthesis of thiazolet, TCA cycle V and incomplete reductive TCA cycle, associated with decreased *Akkermansia* and *Eubacterium coprostanoligenes* abundance as compared to the Sham3 group. Compared with the LR3 group, mice in the liver repair phase (LR14 group) exhibited upregulation of GDP-mannose biosynthesis and the urea cycle, associated with increased *Candidatus arthromitus* and *Mucispirillum* abundance, as well as downregulation of the pathway of chorismate metabolism and biosynthesis of cob(II) yrinate a,c-diamide, (Kdo)2-lipid A, L-tryptophan and enterobactin. The present study thus revealed the alterations of signal transduction, transcription, cell motility, as well as metabolism of amino acids, lipids, glucose, cofactors and terpenoids, and xenobiotics pathways associated with 50% PH-induced acute liver injury and repair.

These results suggested that acute liver injury may cause microecological dysbiosis, affecting the potential function of the intestinal microbiota (6). At the same time, liver injury induced a compensatory mechanism in the host and the gut microbiota may react to the liver and influence liver repair through changes in microecological function. However, it remains elusive how the intestinal microbiota may be modified to promote the recovery of liver function following hepatectomy. This is a major limitation of the present study and provides a direction for further research.

In conclusion, in the present study, the structural and functional changes of the gut microbiota following 50% PH were investigated. It was indicated that 50% PH reduced the species richness and diversity, caused dysbiosis of the microbiota and altered signal transduction, transcription, cell motility and metabolism of amino acids, lipids and glucose pathways of the intestinal microbiota. A further understanding of the gut-microbiota-liver metabolic network may provide novel strategies for the recovery of patients undergoing liver surgery.

Acknowledgements

The authors would like to thank Mrs. Lei Chen (Medical Information Department of The First Affiliated Hospital, School of Medicine, Zhejiang University), Miss Li Liu (Library of The First Affiliated Hospital, School of Medicine, Zhejiang University) and Mr. Zhuo Yang (LC-Bio Technology Co., Ltd., Hangzhou, China) for their help with data processing, and Dr Han Zhang (Department of Pathology, The First Affiliated Hospital, School of Medicine, Zhejiang University) for his help with the liver histology.

Funding

The present study was supported by the Foundation for Innovative Research Groups of the National Natural Science Foundation of China (grant no. 81721091), the National Natural Science Foundation of China (grant no. 81770645) and the Basic Public Welfare Research Program of Zhejiang Province (grant no. LGF18H030006).

Availability of data and materials

The raw sequencing data and sample information of this study have been submitted to the NCBI Sequence Read Archive under the BioProject accession no. PRJNA678005 (https://www.ncbi.nlm.nih.gov/bioproject/PRJNA678005).

Authors' contributions

YS, ZHH and SSZ conceived and designed the study. YS, YCJ and HL performed the animal experiments. YCJ and HL performed the biochemical analysis and liver histology. FZ, YCJ and HL performed the microecology analysis. YS and YCJ did the data analysis. YS drafted the manuscript. YS and HL confirmed the authenticity of the raw data. SSZ and ZHH supervised the study. All authors read and approved the final manuscript.

Ethics approval and consent to participate

The Animal Experimental Ethics Committee of the First Affiliated Hospital, School of Medicine, Zhejiang University (Hangzhou, China) approved this study (approval no. 2019-1086).

Patient consent for publication

Not applicable.

Competing interests

The authors declare that they have no competing interests.

References

1. Usami M, Miyoshi M and Yamashita H: Gut microbiota and host metabolism in liver cirrhosis. World J Gastroenterol 21: 11597-11608, 2015.
2. Yang R, Xu Y, Dai Z, Lin X and Wang H: The immunologic role of gut microbiota in patients with chronic HBV infection. J Immunol Res 2018: 2361963, 2018.
3. Lu H, Wu Z, Xu W, Yang J, Chen Y and Li L: Intestinal microbiota was assessed in cirrhotic patients with hepatitis B virus infection. Intestinal microbiota of HBV cirrhotic patients. Microb Ecol 61: 693-703, 2011.
4. Jun DW, Kim KT, Lee OY, Chae JD, Son BK, Kim SH, Jo YJ and Park YS: Association between small intestinal bacterial overgrowth and peripheral bacterial DNA in cirrhotic patients. Dig Dis Sci 55: 1465-1471, 2010.
5. Usami M, Miyoshi M, Kanbara Y, Aoyama M, Sakaki H, Shuno K, Hirata K, Takahashi M, Ueno K, Hamada Y, *et al*: Analysis of fecal microbiota, organic acids and plasma lipids in hepatic cancer patients with or without liver cirrhosis. Clin Nutr 32: 444-451, 2013.
6. Dong X, Feng X, Liu J, Xu Y, Pan Q, Ling Z, Yu J, Yang J, Li L and Cao H: Characteristics of intestinal microecology during mesenchymal stem cell-based therapy for mouse acute liver injury. Stem Cells Int 2019: 2403793, 2019.
7. Tremaroli V and Bäckhed F: Functional interactions between the gut microbiota and host metabolism. Nature 489: 242-249, 2012.
8. Cani PD: Metabolism in 2013: The gut microbiota manages host metabolism. Nat Rev Endocrinol 10: 74-76, 2014.
9. Maynard CL, Elson CO, Hatton RD and Weaver CT: Reciprocal interactions of the intestinal microbiota and immune system. Nature 489: 231-241, 2012.
10. Viaud S, Saccheri F, Mignot G, Yamazaki T, Daillère R, Hannani D, Enot DP, Pfirschke C, Engblom C, Pittet MJ, *et al*: The intestinal microbiota modulates the anticancer immune effects of cyclophosphamide. Science 342: 971-976, 2013.
11. Fukuda S, Toh H, Hase K, Oshima K, Nakanishi Y, Yoshimura K, Tobe T, Clarke JM, Topping DL, Suzuki T, *et al*: Bifidobacteria can protect from enteropathogenic infection through production of acetate. Nature 469: 543-547, 2011.
12. Schroeder BO and Bäckhed F: Signals from the gut microbiota to distant organs in physiology and disease. Nat Med 22: 1079-1089, 2016.
13. Lin R, Zhou L, Zhang J and Wang B: Abnormal intestinal permeability and microbiota in patients with autoimmune hepatitis. Int J Clin Exp Pathol 8: 5153-5160, 2015.
14. Moen AEF, Lindstrøm JC, Tannæs TM, Vatn S, Ricanek P, Vatn MH and Jahnsen J; IBD-Character Consortium: The prevalence and transcriptional activity of the mucosal microbiota of ulcerative colitis patients. Sci Rep 8: 17278, 2018.
15. Michalopoulos GK: Liver regeneration. J Cell Physiol 213: 286-300, 2007.
16. Michalopoulos GK: Hepatostat: Liver regeneration and normal liver tissue maintenance. Hepatology 65: 1384-1392, 2017.
17. Flye MW and Yu S: Augmentation of cell-mediated cytotoxicity following 50% partial hepatectomy. Transplantation 49: 581-587, 1990.

18. Cao H, Yu J, Xu W, Jia X, Yang J, Pan Q, Zhang Q, Sheng G, Li J, Pan X, *et al*: Proteomic analysis of regenerating mouse liver following 50% partial hepatectomy. Proteome Sci 7: 48, 2009.
19. Brandt HH, Nißler V and Croner RS: The influence of liver resection on intrahepatic tumor growth. J Vis Exp 110: e53946, 2016.
20. Fadrosh DW, Ma B, Gajer P, Sengamalay N, Ott S, Brotman RM and Ravel J: An improved dual-indexing approach for multiplexed 16S rRNA gene sequencing on the Illumina MiSeq platform. Microbiome 2: 6, 2014.
21. Callahan BJ, McMurdie PJ, Rosen MJ, Han AW, Johnson AJ and Holmes SP: DADA2: High-resolution sample inference from Illumina amplicon data. Nat Methods 13: 581-583, 2016.
22. Blaxter M, Mann J, Chapman T, Thomas F, Whitton C, Floyd R and Abebe E: Defining operational taxonomic units using DNA barcode data. Philos Trans R Soc Lond B Biol Sci 360: 1935-1943, 2005.
23. Bolyen E, Rideout JR, Dillon MR, Bokulich NA, Abnet CC, Al-Ghalith GA, Alexander H, Alm EJ, Arumugam M, Asnicar F, *et al*: Author correction: Reproducible, interactive, scalable and extensible microbiome data science using QIIME 2. Nat Biotechnol 37: 1091, 2019.
24. Caporaso JG, Kuczynski J, Stombaugh J, Bittinger K, Bushman FD, Costello EK, Fierer N, Peña AG, Goodrich JK, Gordon JI, *et al*: QIIME allows analysis of high-throughput community sequencing data. Nat Methods 7: 335-336, 2010.
25. Segata N, Izard J, Waldron L, Gevers D, Miropolsky L, Garrett WS and Huttenhower C: Metagenomic biomarker discovery and explanation. Genome Biol 12: R60, 2011.
26. Langille MG, Zaneveld J, Caporaso JG, McDonald D, Knights D, Reyes JA, Clemente JC, Burkepile DE, Vega Thurber RL, Knight R, *et al*: Predictive functional profiling of microbial communities using 16S rRNA marker gene sequences. Nat Biotechnol 31: 814-821, 2013.
27. Parks DH, Tyson GW, Hugenholtz P and Beiko RG: STAMP: Statistical analysis of taxonomic and functional profiles. Bioinformatics 30: 3123-3124, 2014.
28. Liu HX, Rocha CS, Dandekar S and Wan YJ: Functional analysis of the relationship between intestinal microbiota and the expression of hepatic genes and pathways during the course of liver regeneration. J Hepatol 64: 641-650, 2016.
29. Crespo-Piazuelo D, Estellé J, Revilla M, Criado-Mesas L, Ramayo-Caldas Y, Óvilo C, Fernández AI, Ballester M and Folch JM: Characterization of bacterial microbiota compositions along the intestinal tract in pigs and their interactions and functions. Sci Rep 8: 12727, 2018.
30. Samul D, Worsztynowicz P, Leja K and Grajek W: Beneficial and harmful roles of bacteria from the Clostridium genus. Acta Biochim Pol 60: 515-521, 2013.
31. Masumoto S, Terao A, Yamamoto Y, Mukai T, Miura T and Shoji T: Non-absorbable apple procyanidins prevent obesity associated with gut microbial and metabolomic changes. Sci Rep 6: 31208, 2016.
32. Jiao X, Wang Y, Lin Y, Lang Y, Li E, Zhang X, Zhang Q, Feng Y, Meng X and Li B: Blueberry polyphenols extract as a potential prebiotic with anti-obesity effects on C57BL/6 J mice by modulating the gut microbiota. J Nutr Biochem 64: 88-100, 2019.
33. Reunanen J, Kainulainen V, Huuskonen L, Ottman N, Belzer C, Huhtinen H, de Vos WM and Satokari R: Akkermansia muciniphila adheres to enterocytes and strengthens the integrity of the epithelial cell layer. Appl Environ Microbiol 81: 3655-3662, 2015.
34. Belzer C and de Vos WM: Microbes inside-from diversity to function: The case of Akkermansia. ISME J 6: 1449-1458, 2012.
35. Anhê FF, Roy D, Pilon G, Dudonné S, Matamoros S, Varin TV, Garofalo C, Moine Q, Desjardins Y, Levy E and Marette A: A polyphenol-rich cranberry extract protects from diet-induced obesity, insulin resistance and intestinal inflammation in association with increased Akkermansia spp. population in the gut microbiota of mice. Gut 64: 872-883, 2015.